Estimation of Surface Soil Moisture from Agricultural Lands using Multi-Spectral Optical Satellite Data: A Study of Bhagwanpur-I CD Block, East Medinipur, West Bengal, India.

Goutam Kumar Das*

Department of Earth System Science, Vidyasagar University, India
*Corresponding Author's email: goutamrs2014@gmail.com

Abstract

The spatiotemporal fluctuation of Surface Soil Moisture theatres a crucial important for prediction of weather, scarcity of water, modeling of hydrological cycle, agricultural managing and making strategy. Optical remote sensing has demonstrated significant promise for precise surface soil moisture estimate. The aimed study estimated moisture content in the upper layer of the agricultural fields using Landsat 8 OLI, Sentinel-2A multi-spectral satellite data as well as TVDI (Temperature Vegetation Dryness Index). The spatial resolution of the Landsat OLI and Sentinel-2A photos used in this investigation was 30 m and 10 m, respectively. The spectral Thermal Infrared (TIR 10.9 µm), TIR (10.9µm) and along with the Short-Wave-Infrared (SWIR 2.2 µm) band of the Landsat 8 and the Shore-Wave-Infrared (SWIR 2.2 µm) band of sentinel 2B satellite imagery was utilized to estimate how moist was topsoil of the agricultural lands. The acquired and compared to remotely model-based soil moisture and in-situ soil moisture. In a depth of 10 cm below the surface, the field-based soil moisture was measured. The use Normalized Difference Vegetation Index (NDVI) and Land Surface Temperature (LST), the Temperature Vegetation Dryness Index (TVDI) was created to estimate moisture content. The reflectance values of the TVDI are shown over the study area generally are low, with the values ranging from -0.07 to 1.37. The statistical tests of TVDI values and Gravimetric soil moisture values presented a positive correlation with RMSE= 0.17 for the date 23.04.2021. The results of the study area can give to better hydrological modeling, management of agriculture, policy making. However, further research is required to validate the methodology over a larger geographical area and to evaluate the accurateness of the assessed the SSM at the various depths of the soil.

Keywords: Surface Soil Moisture, Normalized Difference Vegetation Index, Land Surface Temperature, Temperature Vegetation Dryness Index.

Introduction

Surface Soil Moisture content theatres a crucial character in the hydrological techniques by way of it protect the separating to the run-off and infiltration. Accurate estimation of agriculture and vegetation growth can improve the accuracy of hydrological models besides predictions of water resources availability (Anguela et al., 2008; Kornelsen and Coulibaly, 2013; Bertoldi et al., 2014). The moisture content in the upper layer of soil, typically the first 5-10 cm of soil, and his theatrical important part in many environmental processes. Surface soil moisture is used to predict weather conditions, including precipitation, and it also theatres a part in the liveliness balance among the earth surface and atmosphere through evapo-transpiration (Du et al., 2010; El Hajj et al., 2016; Kurum et al., 2009; Şekertekin et al.,

2016; Srivastava et al., 2015; Zribi et al., 2016). Wang et al., 2021, evaluated the uses the Gravimetric method to the amount water content in a field experiment. The research showed that the Gravimetric method provided accurate and reliable measurements of water in the soil, that's used to optimize cropping schedules and improve crop yields. Bogdan Ruszczak et al., 2022, evaluated the accurateness of the Gravimetric method in measuring the amount of water in different soil types of the several times. The gravimetric method, where the percentage of dry soil weight is given, is useful to control the soil moisture content of the soil from the difference in weight before and after drying. With this technique, a soil sample weighing around 100 g is obtained and baked for 30 minutes at a temperature between 90°C and 105°C, or until it reaches a consistent weight (Syed Muhammad Zubair Younis and Javed Iqbal, 2015). (Syed Muhammad Zubair Younis and Javed Iqbal, 2015) the difference between the soil samples before and after drying weights is recorded. The percentage of soil moisture is intended through the following equation:

$$\% \text{ of soil moisture} = \left[\left(\frac{\text{Wet weight} - \text{Dry weight}}{\text{Dry weight}}\right)\right] * 100 \qquad \text{Eq. (1)}$$

Spectral bands of Visible and infrared remote sensing methods depend on the interaction among the solar radiation and surface soil to infer soil moisture content (Batlivala and Ulaby, 1977; Seneviratne et al., 2010; Petropoulos et al., 2015). Sadeghi et al. (2017) used remotely sense satellite data and vegetation indices towards the study. The vegetation catalogues, as an NDVI (Normalized Difference Vegetation Index), are normally used to identify water stress and monitor vegetation. The visible and NIR spectral information from remote sensing is deliberated by the NDVI, which is adaptable to changes in vegetation intensity. Rao et al. (1993) deliberates the association among vegetation lands and NDVI, as healthy as root zone soil moisture. They found that there was a direct relationship among root zone and NDVI surface soil moisture, but that the strong point of the relationship diverse dependent on the type of crops being studied. LST is typically estimated from the thermal emission measured by thermal infrared sensors on remote sensing platforms. In addition, NDVI is also evaluated using the surface's reflectance of red and near-infrared wavelengths, which are a portion of the electromagnetic spectrums optical range (Amato et al., 2015; Hammam and Mohamed 2018). Soil moisture can affect the thermal inertia of the soil, but soil with greater moisture content will have a lower thermal persistence.

Materials and Methods

Study Area:

Bhagwanpur 1 CD block is a predominantly rural area with a significant population engaged in agriculture-based activities. The study area is located in the Purba Medinipur district of West Bengal, India, and is bounded by the Paschim Medinipur district to the west, the Moyna CD block to the north, the Chandpur CD block to the east, and the Bhagwanpur-II and Patashpur-I CD block to the south. Physically, the study area is located between 22º0′16.46″N to 22º10′40.71″ N latitude and 87º40′19.76″E to 87º50′18.31″E longitude, the geographical land area approximately 182.99 km2, and the population is 234,432, of which 222,677 were rural and 11,755 were urban as per the 2011 census. The block is divided into

164 inhabited villages, 167-gram sansads (village councils), and 10 GP (Souvik Mondal et al., 2019) and its physiographic soil, vegetation, geology, and drainage system is yet to be described. The moist soil has a high water-holding capacity and are typically found in low-lying areas and alluvial plains. They are characterized by high soil moisture levels throughout the year, especially during the monsoon season and dry soil typically found in upland areas through well-drained soils. They are characterized by low soil moisture levels throughout the year, especially during the dry season. So, soil moisture is significant to messages that these regimes may vary depending on the specific location and site characteristics within Purba Medinipur district. Therefore, it is essential to conduct site-specific assessments to understand this soil moisture regime in a specific region (Maiti et al., 2013).

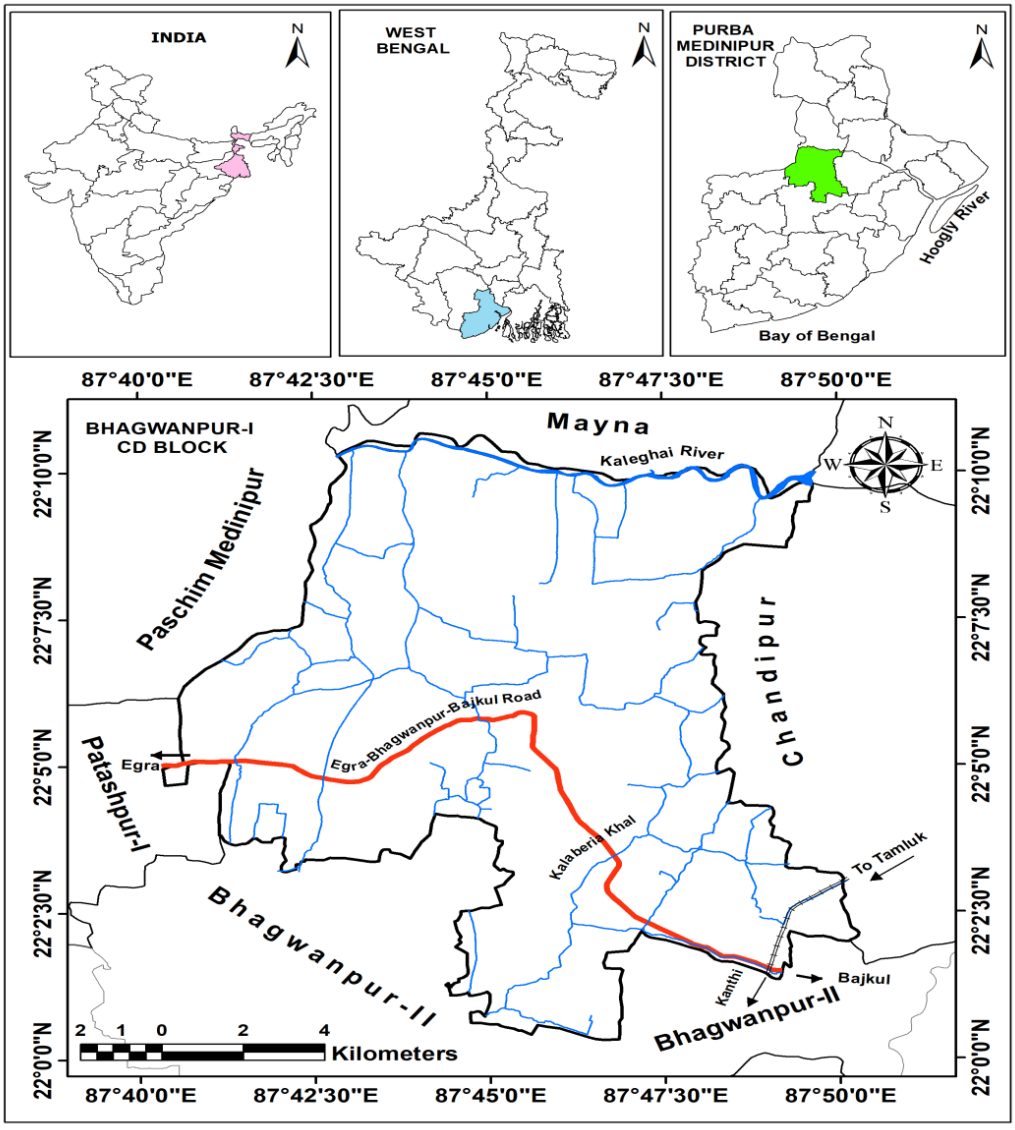

Fig. 1 Location map of the study area.

Datasets:

Field data collection:

Empirical survey was conducted in the CD block of Bhagwanpur-I to collect soil samples. The water supply intervals and 52 land parcels existed selected for soil sample collection, and the dimensions of land parcels were measured and presented in Table 1. The soil

samples were collected in the tighter air bag since these parcels on 24.03.2021. The corresponding latitude and longitude locations of the soil sample collection points were measured using GPS with 1-meter accuracy.

Satellite data used and Pre-processing:

Landsat 8 (OLI) satellite image: Landsat 8 (OLI) satellite image information is a widely used source for remote sensing studies. In this work, the moisture content of the agricultural field was evaluated using Landsat-8 OLI data. The Landsat 8 sensor provides multi-spectral imagery with 11 spectral bands, counting two NIR bands. The spatial resolution of OLI data is 30 meters, although the TIRS sensor delivers thermal imagery with a ground resolution of 100 meters, which was resampled to 30 meters for this study. The Communal method mainly used to resample remote sensing data a bi-linear interpolation. Using a weighted average of the neighboring pixels in the original image, bi-linear interpolation calculates the values of each new pixel in the resampled image. The United States Geological Survey (USGS) authorized data downloading web-portal (https://earthexplorer.usgs.gov/) was used to get the Landsat-8 OLI data for April 25, 2021.To avoid cloud contamination, images with minimal cloud coverage were selected, which the study area's path 138 and raw 45 both cover.

Sentinel-2B Data Availability: In the study area, Multispectral Instrument (MSI) was used to identify the permanent water body, vegetation, build up, and crop land. We can use USGS open-source data portal to download 25-April-2021 ("S2A_MSIL1C_20210424T043701_N0300_R033_T45QWE_20210424T064545"). Sentinel-2A and 2B are both part of the European Union Copernicus platform, and they deliver high spatial multispectral imagery with a chronological break of 5 days. Sentinel-2B have covered the visible, NIR and SWIR regions with the 13 spectral bands, and ground coverage of 10, 20, and 60 meters depending on the band. As an illustration, the spatial resolution of the visible and NIR bands is 10 meters, whereas the spatial resolution of the SWIR bands and the four vegetation red edge bands is 60 meters. The spatial resolution of the coastal aerosol, water vapor, and SWIR cirrus bands is 60 meters. In this study sentinel-2B Level-1C (L1C) data from April 25th, 2021 was downloaded to the data hub of the European Space Agency (https://scihub.copernicus.edu/dhus/#/home).

Landsat 8 and Sentinel 2 B satellite imagery pre-processing:

The methods used for calculating sensor radiance for Landsat 8 satellite imagery are as following:

$$\mathrm{L} = \left[\left\{\left(\frac{Lmax - Lmin}{\mathrm{QCalmax} - \mathrm{QCalmin}}\right) * (\mathrm{QCal} - \mathrm{Qcalmin})\right\} + \mathrm{Lmin}\right] \qquad \text{Eq. (2)}$$

Where, the radiance value is Maximum spectral radiance Lmax, Lmin is the minimum spectral radiance, maximum calibrated quantization level is QCalmax and QCalmin is short for qualified quantization.

This formula takes into account the range of values for the calibration level of quantization (QCal), the minimum and maximum spectral values, and a constant offset term (Lmin). The spectral radiance values are affected by atmospheric correction are required to remove

these effects and obtain accurate reflectance values and land surface temperature (LST) measurements. The radiance values obtained from Equation (2), were used for atmospheric alteration to determine the Red, NIR, and SWIR band reflectance values, in addition for scheming the LST or Land Surface Temperature values to the thermal-infrared spectral band of Landsat 8 (OLI) imagery. The Level-1C products generated from sentinel-2B data are pre-processed and come using the values of top-of-atmosphere reflectance, and atmospheric correction was performed consuming the SNAP device in the sentinel application platform. The Normalized Difference Vegetation Index (NDVI), which was predicted by Rouse et al. (1974), is a commonly used measure of vegetation intensity, and red and NIR bands to use for calculating spectral reflectance.

NDVI = (NIR-RED) / (NIR+RED) Eq. (3)

Where, NDVI has been widely used for vegetation intensity and it's based on the association with the spectral reflectance values of NIR and Red bands. While it is able to deliver information of plants healthiness and density, it is not directly related to soil moisture content. Therefore, combining NDVI and LST data can help differentiate between areas with similar vegetation cover but different soil moisture conditions. The scatter plot of LST and NDVI values can make known the soil-vegetation patterns, and the distribution of the scatter plot can help extract the Soil Dryness Index Composite (SDIC) that performed for the evaluation of moisture content on the earth's surface.

The Top-of-atmosphere's spectral radiance changed

The DN values captured by the satellite sensors need to be converted to TOA radiance values for further analysis. This conversion is done using algorithms provided by the USGS website of the Landsat 8 missions. The conversion algorithm takes into account the calibration coefficients provided by the satellite manufacturers and the radiance of the sun at the moment of acquisition. The values responsible for TOA radiance are then used for atmospheric correction and other analysis. The radiometric correction was completed in the Landsat 8 (OLI) bands using the Equation (5) in Arc GIS. Software band math function.

$L\lambda = M*P+A$ Eq. (5)

Where, $L\lambda$=Spectral radiance (w/cm2μm), M is among a radiance multiplication scaling factor, A is radiance additive scaling factor for the spectral band, P is pixel values.

The equation (3) is performed to determine the Normalized Difference Vegetation Index (NDVI) for images captured by the satellites Landsat 8(OLI) and Sentinel 2B, for Landsat 8 (OLI), the spectral bands 5 and 4 stand for the NIR, and Red bands, respectively, while for Sentinel 2B, the spectral bands 4 and 3 represent the equivalent. For using the radiance value (L) and (equation (2)), Brightness Temperature (kelvin) was derived from the Land Surface Temperature (LST) of the Landsat 8 imagery.

$$T_B = \frac{K^2}{in\left(K^1/_2 + 1\right)} \qquad Eq.(6)$$

Where, T_B is Brightness Temperature, L=Radiance obtain from (Equation (1)), K_1 andK_2=Calibrated constant values get to the image metadata, K1 and K2 constant of band 10 is 774.8853 and 1321.0789, respectively. The function of Land Surface Temperature (LST) of any region depends on the thermal emissivity for the vegetation function are fallows:

$$P_V = \left(\frac{\text{NDVI} - \text{NDVImin}}{\text{NDVImax} - \text{NDVImin}}\right)^2 \qquad Eq.(7)$$

Where, Pv stands for the vegetation functions, and NDVImax and NDVImin are the minimum and maximum NDVI values. Sovbrino et al. (2004) used the Pv values to get the value of Emissivity (E).

$$E = 0.004 * Pv + 0.986. \qquad Eq.(8)$$

The finally, LST was calculated using Equation (2).

$$LST = \frac{\text{T}_\text{B}}{1 + \frac{(0.00115 * \text{T}_\text{B})}{1.4388} * \text{In(E)}} \qquad Eq.(9)$$

It is not possible to directly establish a direct association among the NDVI and LST for Sentinel-2B imagery since it does not have a thermal band. However, if the assumption is made that the NDVI and LST acquired from Landsat 8 (OLI) data of the similar region and time period have a direct relationship, then it may be possible to use this relationship to estimate LST values for the Sentinel-2A NDVI data. This is constructed on the statement that the vegetation conditions for the two datasets are similar. It is important to note that this approach may have some limitations and uncertainties due to differences in the spatial and spectral resolution, atmospheric conditions, and other factors that can affect the relationship between NDVI and LST.

DEM data per-processing: Pre-process the DEM data we can use some G.P.S survey in his region to collect elevation data and generate it in the DEM with latitude, longitude in particular away. Then IDW in all data set and generate a DEM for Surface Soil Moisture (SSM) estimation. The north to south cross section line has a total length of 16.09 km, with a maximum slope ranging from 1°45'18" to 1°50'42". The average slope of this cross-section line is 0°24'18", and the minimum elevation value is 0.914 meters, while the maximum elevation value is 9.7536 meters. On the other hand, the west to east cross section line has a total length of 12.15 km, with a maximum slope ranging from 1°53'24" to 1°56'6". The average slope of this cross-section line ranges from 0°24'18" to 0°27'0". The minimum elevation value of this cross-section line is 2.45 meters, while the maximum elevation value is 8.53 meters (G.P.S survey, Google Earth image and Alos Palser DEM).

GPS Field Survey with validation: As geospatial technology-based product is the foundation of natural resource management and decision-making process; it is very much useful for mitigating the error and accuracy assessment by using some algorithm. Accuracy is

considered to truthiness of the result. Validated the result we can use the field survey; it is very much important for accuracy assessment. GPS base Survey is validated the ground data to the image. The ground collection point is shown in figure (2).

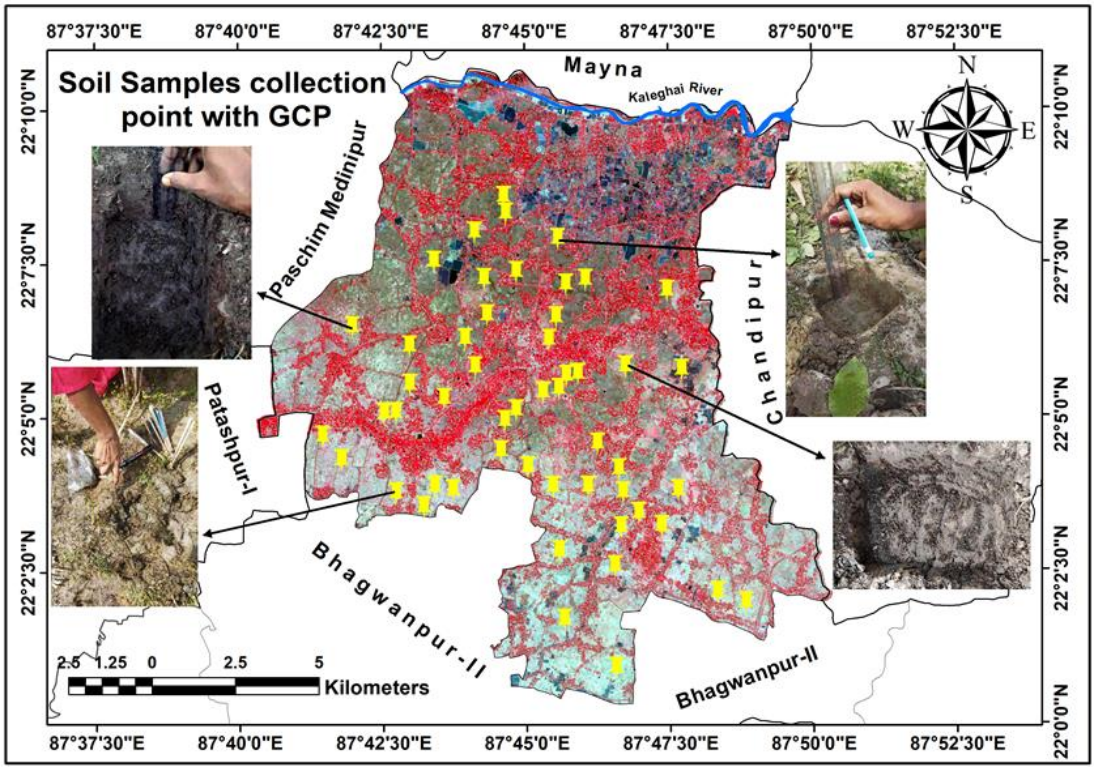

Fig. 2 Soil Samples and GCP collection point of the study area.

Methods:

Field Study: Field work was done 25th April 2021 to collected major soil samples data. The measuring surface soil moisture using direct from the soil samples is a reliable technique. The randomized sampling procedure is also a good approach to ensure representative soil samples. The collection of 52 soil samples at 0-10 cm depth, through a width of 110 cm and length is 18 cm is sufficient to obtain a good spatial distribution of soil moisture data (figure-8). Geo-referencing the sampling points using a handheld GPS system is also important to accurately locate the sampling points in the study area. It's also good to hear that the soil samples were reassigned to a soil laboratory for further analysis of surface soil moisture.

Gravimetric methods use for Surface Soil Moisture: Gravimetric method is a conventional technique for measuring soil moisture content. These methods, a recognised weight of the soil samples is taken and then dried in a shiver machine at a quantified temperature for a stated period of time till all the water has been disappeared from the soil. The dry weight of the soil is then measured and by subtracting the dry weight of the original soil mass and dividing the result by the dry weight, the moisture content of the soil is taken into explanation (Syed Muhammad Zubair Younis and Javed Iqbal, 2015).). In the study area, soil samples were taken using a gravimetric technique at a depth of 1 to 5 cm. After collection, the soil samples were transformed to a soil laboratory and all samples were dried in an oven

at a temperature range of 85℃-110℃ for 30 minutes. The soil moisture content was calculated using the gravimetric method, which provides a perfect measured of content of soil moisture at a specific depth. These measurements can be used to validate and calibrate remotely sense used for mapping surface soil moisture. This method involves collecting soil samples from the field, drying them in an oven, and measuring sample weight before and after drying to calculate the soil moisture content. The distribution of our test location of surface soil moisture is mostly affected by irrigation and rainfall patterns. Therefore, it is important to collect soil samples simultaneously with the satellite image acquisition to ensure that the data accurately indicates the moisture levels in the soil's top layer. By averaging the gravimetric reading from various soil samples taken from the test location, the average values of the surface soil moisture content may be intended.

$$\text{Gravimetric Soil Moisture(Sg)} = \frac{\text{Ws} - \text{Wd}}{\text{Wd}} * 100 \quad (11)$$

$$\text{Builk Density (Pb)} = \frac{\text{Ws}}{\text{V}} \quad (12)$$

$$\text{Valumetric Soil Moisture (Sv)} = \text{Sg} * \text{Pb} \quad (13)$$

Where, Ws is weight of soil moisture, Wd is weight of dry soil samples is volumes of soil samples.
The Gravimetric Soil Moisture (Sg) value calculated for each test site range between.

Estimation of Soil Moisture through the Remote Sensing data: Temperature Vegetation Dryness Index (TVDI) is a method that uses Landsat-8 imagery to assess surface soil moisture content through the combining optical datasets such as; visible, infrared and thermal bands. Normalized Difference Vegetation Index (NDVI), and Land Surface Temperature (LST) which is utilized plants and water stress, are the foundation of the TVDI techniques. The link between thermal and visible/NIR data is used in the TVDI method to map soil moisture. The distribution of pixel values in Ts-NDVI space is interpreted to identify a huge space of the soil water content and the triangle-shaped greenery that surrounds it. This triangle is designed for decreased surface temperature as increased vegetation cover. By using a scatter plot among the LST and NDVI space and TVDI techniques, which are closely related to surface temperature and moisture.

Theatrical background NDVI and LST Spectral Space for estimation of soil moisture: The pixel values dropping Lower Left Corner (LLC) points, were placed low NDVI and LST, stand made patches of moist, exposed soil. The amount of pixels that were identified in the Upper left Corner (ULC) as dry, bare soil regions had high LST and low NDVI. The pixels with low LST and high NDVI in the Lower Right Corner (LRC) originate from areas of think vegetation with low soil moisture content. Therefore, distinguishing the wet and dry edges from the NDVI and LST spectral space is important from a scientific standpoint since these edges are crucial for determining the minimum and maximum LST inconsistency for specific NDVI values, as shown in figure (3).

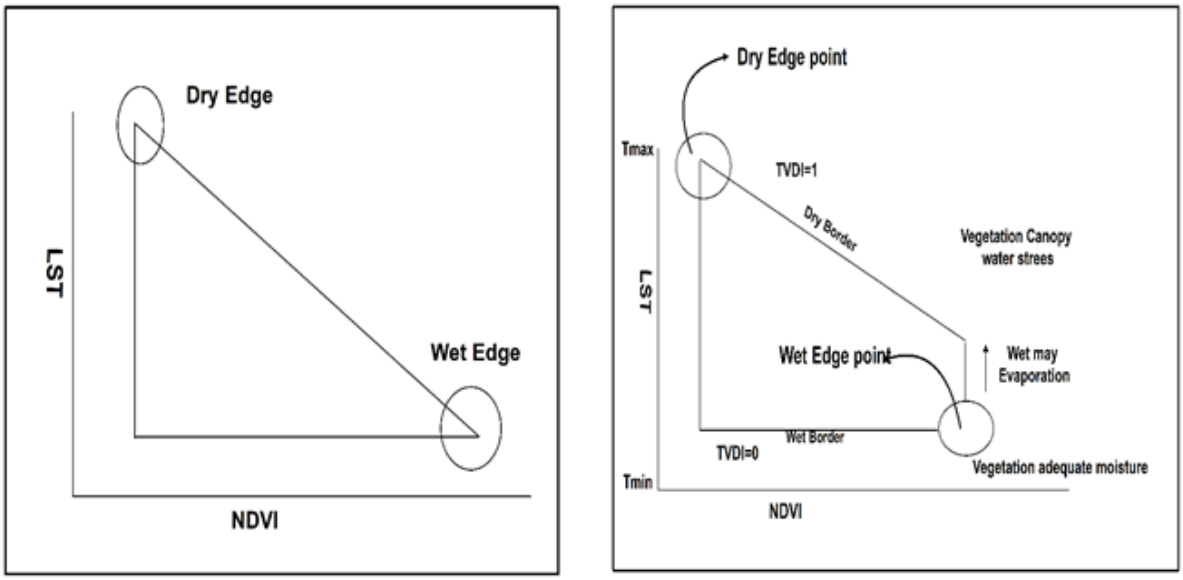

Fig. 3 Theoretical Background of Soil Moisture content used LST Spectral Space and NDVI Estimation.

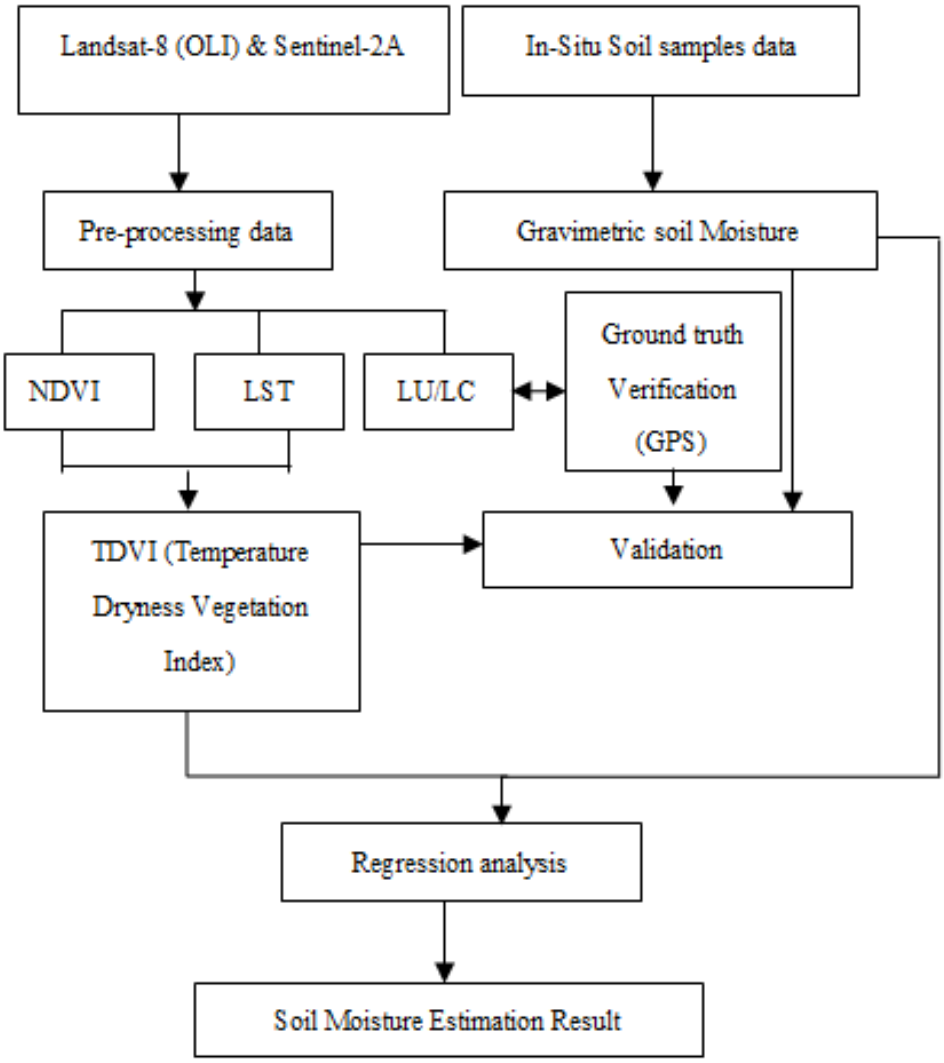

Fig. 4 Methodological flow chart of the study.

Computation of TVDI: The slope (b) and intercept (a) of the dry edge and wet edge of the surface were used to determine the LSTmax and LSTmin, two important edge numbers. Equation 14a and 14b.The LST of dry and wet soil, respectively, is what LSTmax and LSTmin are made up of. The subsequent equation was performed to determine the maximum and minimum LST for the dry edge and wet edge of the surface.

$$\mathrm{LSTmax} = a1 + b1 * NDVI \quad \text{Eq. (14a)}$$

$$\mathrm{LSTmin} = a2 + b2 * NDVI \quad \text{Eq. (14b)}$$

Where, NDVI stands for the Normalized Difference Vegetation Index, the intercepts of the dry and wet edges are (a1) and (a2), respectively, and the slopes of the dry and wet edges are (b1) and (b2), respectively. So, it can determine dry and wet values from the TVDI image. The minimum and maximum LST values can use for calculating the surface soil moisture content of the equation:

TVDI= ((LST-LSTmin)/ (LSTmax-LSTmin)) Eq. (15)

Where, TVDI is Temperate Vegetation Dryness Index, and LST values are obtained from the Landsat 8 (OLI) imagery.

Results and Discussion

The foremost aimed of the study was to use optical multi-spectral images to assess the soil moisture status in the upper layer of the agricultural area in West Bengal's Bhagwanpur-I CD block. The study's finding demonstrated that it is possible to estimate the surface soil moisture content using satellite images from Landsat 8 (OLI) and sentinel 2B. The visible, NIR and thermal infrared dataset were used in the triangulation method for developing the created TVDI map with the Land Surface Temperature (LST) and Normalised Difference Vegetation Index (NDVI). The study found that gravimetric methods provide more accurate soil moisture data compared to indirect measurement methods. The minimum and maximum LST values of wet and dry soil are used to calculate the wet edge and dry edge in the LST-NDVI spectral space.

Soil moisture estimation using optical satellite image: The TVDI method is established in the observation that surface temperature fell as vegetation cover increased. A connection between surface energy and moisture status was built using data from remotely acquired LST (Land Surface Temperature) and NDVI (Normalized Difference Vegetation Index) measurements. From the TVDI image, a vast area of vegetation and soil moisture content was extracted, generating a triangle in the Ts-NDVI space. For estimating the minimum and maximum LST predictability at specific NDVI values, the Ts-NDVI triangle space with dry edge and wet edge of the surface was used. These maximum and minimum LST values are provided were used to evaluate the surface moisture in the upper layer of agricultural areas in the Bhagwanpur-I block of East Medinipur, West Bengal.

NDVI, or Normalized Difference Vegetation Index: The Normalized Difference Vegetation Index (NDVI) is calculated using the reflectance patterns of vegetation leaves in the visible and near-infrared spectra. Because the visible region (0.4–0.7 micrometers) is largely absorbed by the vegetation's healthy chlorophyll concentration, there is little reflection in this region. The calculating NDVI diving among the difference NIR and visible band to the sum of those spectral bands of the satellite image. NIR and red bands are used specifically in the calculation of the Normalized Difference Vegetation Index (NDVI) utilizing Landsat-8 (OLI) images. It can be printed as follows mathematically:

$$NDVI = \frac{NIR - Red}{NIR + Red} \qquad \text{Eq. (16)}$$

Where, the reflectance values in the red band (Landsat 8, band 4) are referred to as Red, and NIR is the reflectance values in the NIR band (Landsat 8, band 5). The formula for calculating NDVI can be used in various software tools, including Erdas Imagine. The NDVI values range between -1 to +1, where values close to +1 and 0 that's specify dense green vegetation and bare soil or rock respectively, another, the values close to the -1 indicate water or snow. In the study, in the studied locations, the NDVI values ranged from 0.02 to 0.54. A study and statistical evaluation of the NDVI-LST model's accuracy in estimating soil water content was conducted. The results showed that the model's ability to forecast soil moisture was enhanced by substituting NDVI for EVI. Figure (5) depicts the NDVI map.

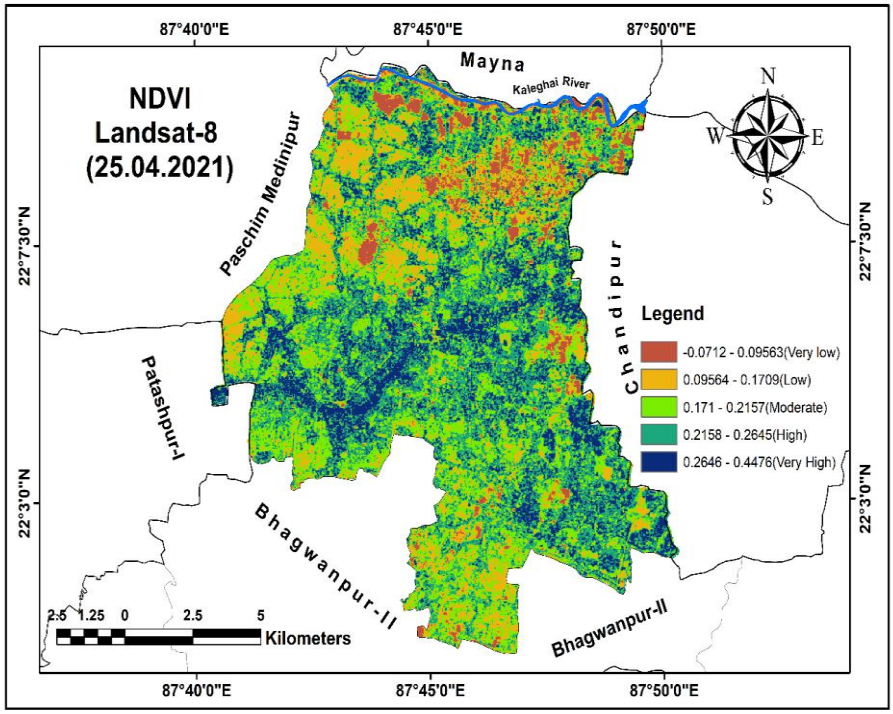

Fig. 5 NDVI of the study area.

The arrangement of the study space into five major NDVI classes based on vegetation intensity is a valuable tool for considerate the distribution of vegetation and its relationship with soil moisture content. The highest vegetation intensity 57.3804 km2 (31.3747%) (Table (1)) was found in the middle and southeastern parts of the study area

where soil moisture content was low. In contrast, the areas with very low and low vegetation intensity 7.3170 km2 and 34.3431 mk2 (4.0008% and 18.7783%) respectively were mainly located in the northern part of the study area where water bodies are present and soil moisture content is high. Moderate and very high vegetation intensity 55.2159 km2 and 28.6308 km2 (30.1912% and 15.6549%), respectively (Table (1)) were found in other parts of the study space. The findings imply that the spread of vegetation in the studied region is significantly influenced by the soil moisture content.

Table 1 Area of NDVI of the study area.

Sl. No.	NDVI values	Area in km2	% of Area in km2
1.	-0.0712 - 0.09563 (Very low)	7.3170	4.0008
2.	0.09564 - 0.1709 (Low)	34.3431	18.7783
3.	0.171 - 0.2157 (Moderate)	55.2159	30.1912
4.	0.2158 - 0.2645 (High)	57.3804	31.3747
5.	0.2646 - 0.4476 (Very High)	28.6308	15.6549
	Total	182.8872	100

LST or Land Surface Temperature: The relationship between the LST and processes including evapotranspiration, surface energy balance, and vegetation development makes it a crucial variable in environmental studies. In the present study, the thermal infrared band (TIR) of a Landsat-8 satellite image was used to compute LST. To determine the LST of the research area, the average values of the two thermal infrared bands (TIR) 10 & 11 bands were taken. Two procedures were taken in order to translate the thermal band's digital numbers (DN) into actual surface temperature measurements. The top of the atmosphere (ToA) radiance values was first converted to the ToA brightness temperature in Kelvin and then back to the ToA radiance values. Using the formula c=k-273.15, the temperature data were finally converted to degrees Celsius. The TIR bands and surface emissivity can be used to estimate LST and surface emissivity, respectively. If both LST and surface emissivity are needed, Landsat-8 (OLI) data can be combined with other satellite data, such as MODIS data, to obtain a higher temporal resolution. However, atmospheric correction is needed to remove the effects of atmospheric water vapor, aerosols, and clouds that can affect TIR radiation. The obtained LST values in the study area ranged from 28.2176°C to 39.0922°C. The temperature map (Figure 6), which depicts the temperature variation among the research locations, was produced using the Arc GIS environment. The study area appears to have been divided into five main groups based on land surface temperature (LST). The largest area was covered by the moderate temperature class, which accounted for 44.4279% (80.7696km2) in the study space (refer to Figure 6). The other classifications, which comprised 5.1876% (9.4311km2), 29.3620% (53.3799km2), 7.7560% (14.1003km2), and 13.2664% (24.1182km2) of the research area, respectively, were very low, low, high, and very high (Table 2). According to the study, the middle and southern portions of the study area, where there was very little water in the soil, were where the majority of the surface temperatures were found. On the other hand, the northern region of the research area, where water bodies predominate and soil water content is very high, is where the low surface temperature was mostly seen.

Table 2 Area of LST of the study area.

Sl. No.	LST values	Area in Km^2	% area in km^2
1	28.22 - 31.29 (Very low)	9.4311	5.1876
2	31.3 - 32.57 (Low)	53.3799	29.3620
3	32.58 - 33.59 (Moderate)	80.7696	44.4279
4	33.6 - 35.04 (High)	14.1003	7.7560
5	35.05 - 39.09 (Very high)	24.1182	13.2664
	Total	181.7991	100

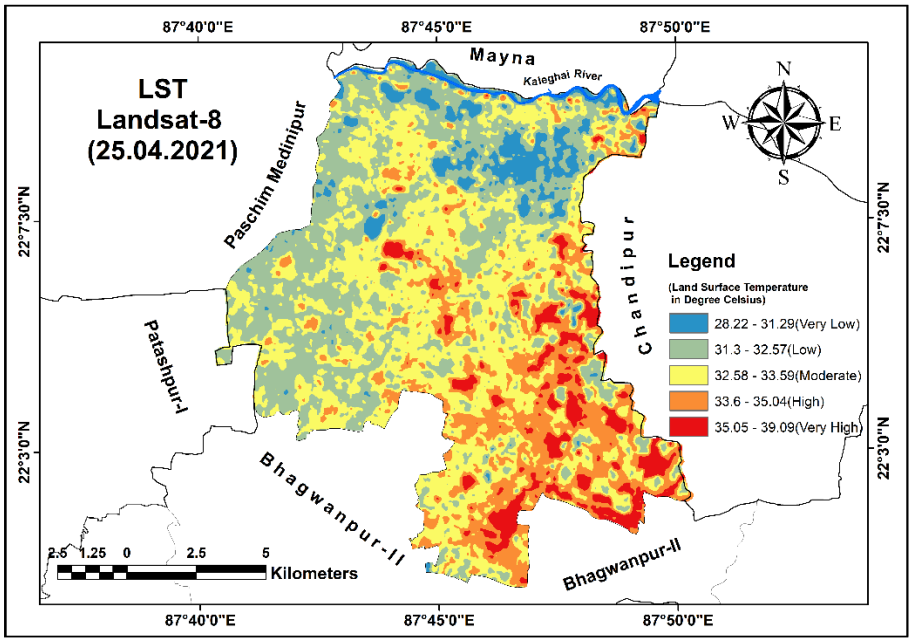

Fig. 6 LST of the study area.

TVDI or Temperature Vegetation Dryness Index: The Temperature Vegetation Dryness Index (TVDI) is computed using the determined values of Land Surface Temperature (LST) and Normalised Difference Vegetation Index (NDVI). The TVDI is a variant of the Vegetation Drought Index (VDI) that takes into account the temperature and vegetation components separately, and it is able to deliver more exact evidence about the severity of drought in vegetated areas. The LST and NDVI readings were plotted against one another in Excel sheets to form the Ts-NDVI space. In order to identify the wet-dry edge of the surface of the research area, regression lines were created to define the upper-lower edge of the triangle. This method helped an image classification of the surface's wet-dry edge based on the distribution of LST and NDVI pixels. Following an analysis of the triangle formed by the distribution plot of LST and NDVI representative the Ts-NDVI planetary data, Inge Sandholt et al. (2002) used this area for the classification of TVDI. The TVDI was considered by subtracting the minimum potential evapotranspiration (PET) from the actual evapotranspiration (ET), which was estimated using the LST and NDVI values. The TVDI values vary from -1 to 1, with destructive values representative wet environments and constructive values representative dry environments. Utilised this space for the TVDI description on behalf of the Ts-NDVI space. Following this, the equation can be used to calculate TVDI.

$$TVDI = \frac{Ts - Tsmin}{Tsmax - Tsmin} \quad \text{Eq. (17)}$$

Where, TVDI is Temperature Vegetation Dryness Index. TS stands for Temperature Surface, while Tsmin and Tsmax represent the minimum and highest land surface temperatures, respectively.

The relationship between the Normalized Difference Vegetation Index (NDVI) and Land Surface Temperature (LST), as well as how they affect the calculation of the Temperature Vegetation Dryness Index (TVDI). There is a strong association among LST and NDVI, with LST declining as NDVI increases during the growing season. This relationship can continue used to conclude the slope of the NDVI-LST curve, which can be successfully determined throughout the growing season of the certain level of NDVI. This information can be useful for estimating in-situ soil moisture, as the derive NDVI incline from image windows remained found to be meaningfully associated with the survey soil moisture, as reported by Xin et al. (2006). This relationship between LST and NDVI is important in the calculation of TVDI, as it takes into account the temperature and vegetation components separately. The TVDI is calculated using a pixel of the LST and NDVI values, as the research area's minimum and highest LST values. The values of TVDI range from 0 to 1, with higher values signifying drier environments is shown in Figure (7).

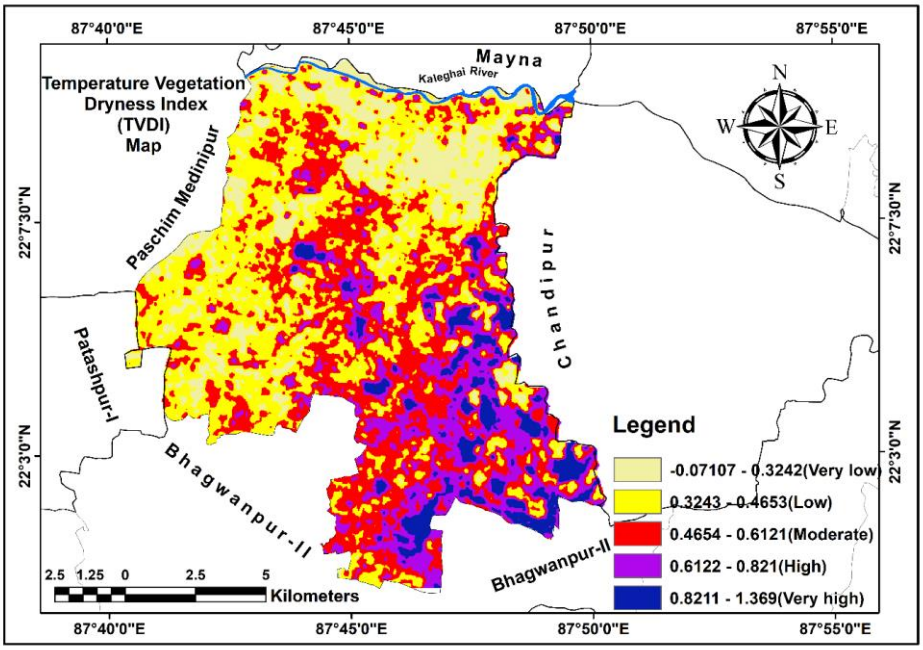

Fig. 7 TVDI map of the study area.

Five classifications can be seen on the TVDI map: low, moderate, high, and very high are the various ranges. Each group is represented in the study region, and the associated percentages are given. The very low and low TVDI values cover 15.4496% (28.2141 km2) and 34.8172% (63.5832 km2) of the study area, respectively. This area is mostly found in the northern-eastern part of the study area where there is more water content in the soil. The third category, moderate TVDI values, accounts for 29.4508% (53.7831 km2) of the study area and is concentrated in the southern and middle regions, where the soil has a moderate amount of water content. The last two categories, high and very high TVDI values,

cover 14.6690% (26.7885 km2) and 5.6133% (10.2510 km2) in the study area, respectively. These TVDI values are mostly found in the southern portion where there is less water in the soil.

Table 3 Area of TVDI of the study area.

Sl. No.	TVDI Values	Area in km2	% of Area in km2
1.	-0.07107 - 0.3242 (Very low)	28.2141	15.4496
2.	0.3243 - 0.4653(Low)	63.5832	34.8172
3.	0.4654 - 0.6121(Moderate)	53.7831	29.4508
4.	0.6122 - 0.821(High)	26.7885	14.6690
5.	0.8211 - 1.369(Very high)	10.2510	5.6133
	Total	182.6199	100

Relationship and spatial variation of the NDVI-LST on April 25, 2021: The spatial variation of high LST and NDVI in the study space. It's stimulating near reminder that LST and NDVI have a favourable connection in south-eastern part of the study area, while a low positive correlation is found in the south-western part. To well appreciate the association among LST and NDVI in the Landsat satellite imagery, the combined values of the LST and NDVI at a 30-meter cover on the ground were designed contradiction each other. This kind of study can offer insights into the relationship between these two factors in Figure (8) as well as patterns and trends in the data.

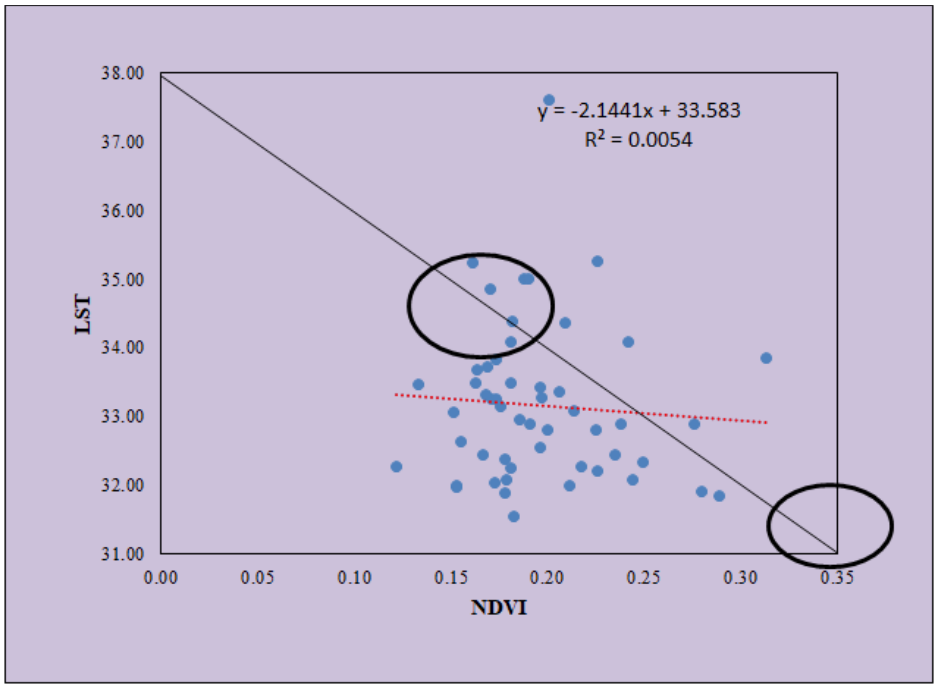

Fig. 8 Land surface temperature and NDVI distribution of sample points.

The validation of Gravimetric Soil Moisture (GSM) content and remote sensing derived soil moisture content: The investigation of the relationship between actual soil moisture and TVDI. It is stimulating that there is the low positive relationship among the TVDI and actual soil moisture content to the Rout Mean Square Errors (RMSE) were documented as 0.175. The TVDI, which was based on a combination of surface temperature and NDVI, was found to be more accurate in regional drought assessment. So, to conclude in the study, recommend the TVDI and dryness index are effective in apprehending the spatial disparity of the condition of soil moisture, for illustration evidenced the final soil moisture map (figure 14).

A SSM map with the classifications of extremely low, low, moderate, high, and very high was created based on the TVDI map. The percentage coverage of each category was calculated. The very low and low SSM values covered 6.006574% (10.9692km2) and 14.19095% (25.9155km2) in study space, respectively, and these are typically located in the southern portion where has very little water in the soil. The central and southern portions, where the soil had moderate water content, were where the moderate SSM values were observed. These areas covered 28.5888% (52.209km2) of the study area. The high and very high SSM values covered 35.39236% (64.6335km2) and 15.82122% (28.8927km2) of the study area, respectively, and where there was a lot of water in the soil in the northwestern, western, northern, and eastern parts of the research region.

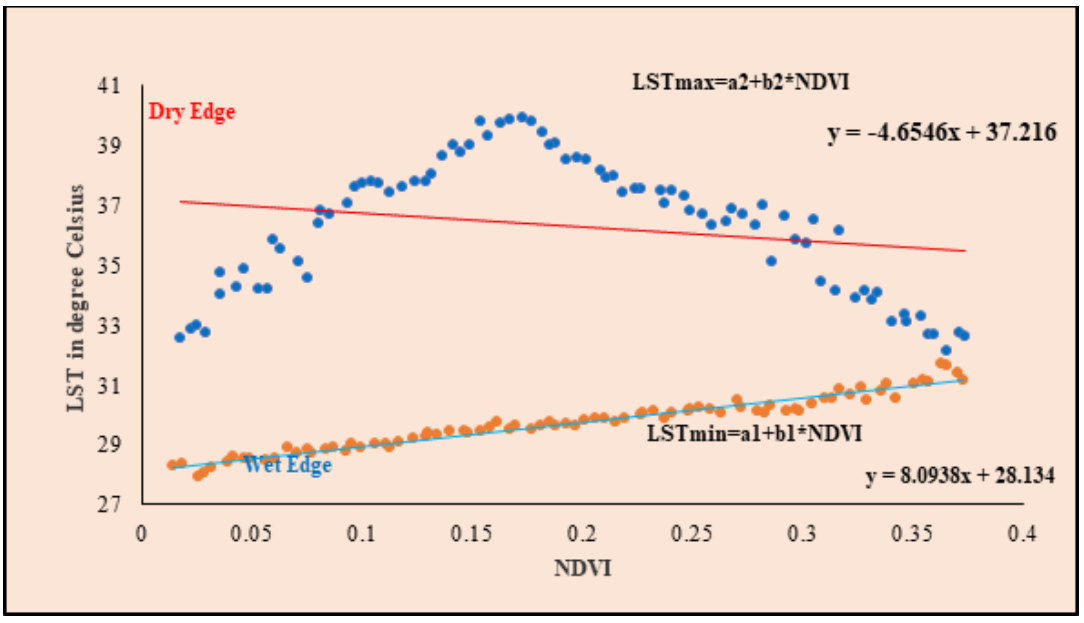

Fig. 9 The study site's dry edge and wet edge of the land and water surfaces are defined by the NDVI-Ts space.

Validation of soil moisture measurements obtained using remote sensing Land Use and Land Cover: A critical step in guaranteeing the correctness and dependability of the acquired data is the validation of LU and LC derived from satellite imagery. The validation process involves comparing the satellite image with ground truth information to assess the level of agreement or disagreement.

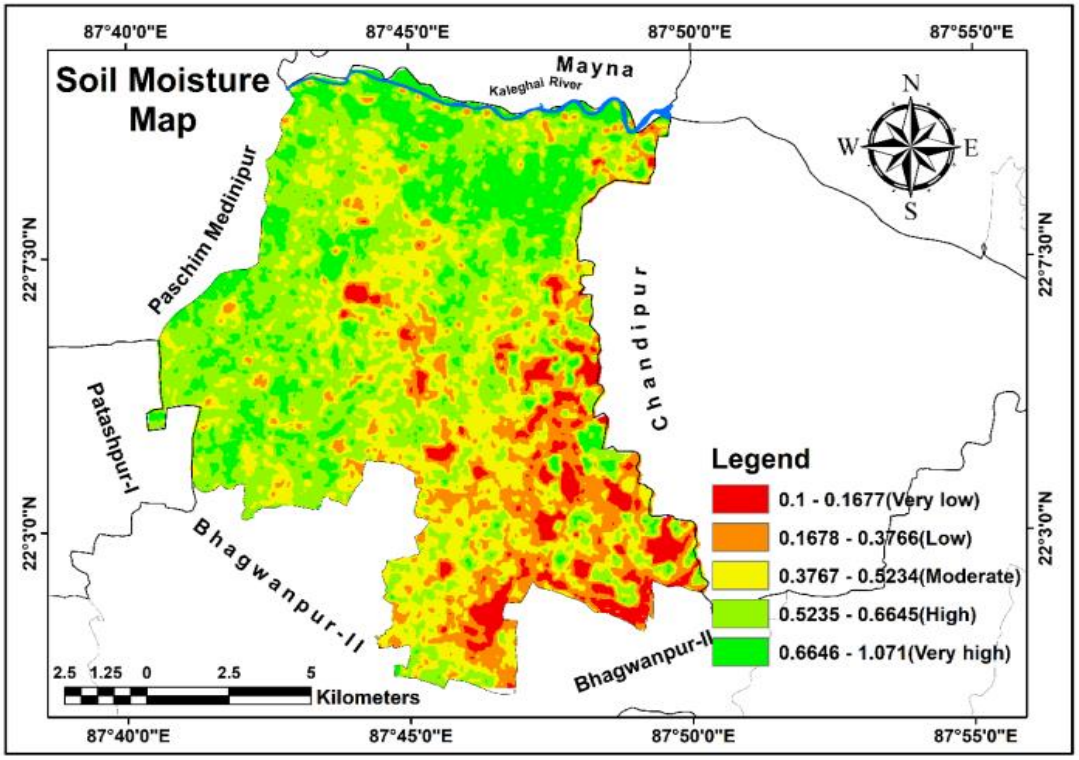

Fig. 10 Soil moisture estimated using remotely sensed data.

Table 4 RMSE between remotely sensed soil moisture and Lab soil moisture.

Sl. No.	Sample Points	In-situ soil moisture (Gravimetric Soil Moisture)	TVDI	Residual	Square of Residual	RMSE
1	S1	0.0638	0.7777	0.2825	0.07980	
2	S2	0.1765	0.6236	0.0910	0.00827	
3	S3	0.1786	0.6604	0.1271	0.01615	
4	S4	0.2658	0.4484	-0.1139	0.01296	
5	S5	0.2346	0.3617	-0.1902	0.03617	
6	S6	0.0638	0.3688	-0.1264	0.01598	
7	S7	0.1549	0.7069	0.1815	0.03294	
8	S8	0.2025	0.8475	0.3062	0.09378	
9	S9	0.0337	0.4250	-0.0602	0.00362	
10	S10	0.0482	0.5370	0.0470	0.00221	
11	S11	0.0877	0.4835	-0.0196	0.00038	
12	S12	0.0976	0.5492	0.0428	0.00183	
13	S13	0.1628	0.5044	-0.0237	0.00056	
14	S14	0.2048	0.2729	-0.2691	0.07244	
15	S15	0.2206	0.2656	-0.2816	0.07932	0.174933
16	S16	0.1447	0.6096	0.0875	0.00766	
17	S17	0.1765	0.4255	-0.1071	0.01146	
18	S18	0.1507	0.5170	-0.0070	0.00005	
19	S19	0.1837	0.6036	0.0686	0.00471	
20	S20	0.1429	0.7062	0.1847	0.03412	
21	S21	0.1647	0.4892	-0.0395	0.00156	
22	S22	0.1228	0.3459	-0.1689	0.02853	
23	S23	0.1159	0.3562	-0.1563	0.02442	
24	S24	0.0964	0.2758	-0.2302	0.05297	
25	S25	0.1364	0.3280	-0.1913	0.03658	
26	S26	0.1236	0.3364	-0.1787	0.03192	
27	S27	0.1628	0.5507	0.0226	0.00051	
28	S28	0.1236	0.4673	-0.0478	0.00228	
29	S29	0.1628	0.7996	0.2716	0.07374	

30	S30	0.1905	1.1967	0.6594	0.43483
31	S31	0.2727	0.6239	0.0593	0.00352
32	S32	0.1625	0.5402	0.0123	0.00015
33	S33	0.1364	0.5710	0.0517	0.00268
34	S34	0.1731	0.5597	0.0282	0.00080
35	S35	0.1892	0.4699	-0.0669	0.00448
36	S36	0.1628	0.3814	-0.1467	0.02152
37	S37	0.1286	0.5736	0.0569	0.00324
38	S38	0.1600	0.3571	-0.1700	0.02890
39	S39	0.1294	0.5235	0.0065	0.00004
40	S40	0.1235	0.6662	0.1512	0.02286
41	S41	0.1071	0.8264	0.3168	0.10035
42	S42	0.0204	0.3504	-0.1304	0.01700
43	S43	0.0526	0.3746	-0.1169	0.01366
44	S44	0.1587	0.3384	-0.1884	0.03548
45	S45	0.0638	0.8041	0.3089	0.09543
46	S46	0.1111	0.4553	-0.0556	0.00310
47	S47	0.0233	0.3953	-0.0864	0.00746
48	S48	0.1628	0.4224	-0.1056	0.01116
49	S49	0.0753	0.4563	-0.0427	0.00182
50	S50	0.1765	0.5379	0.0053	0.00003
51	S51	0.1111	0.5712	0.0603	0.00364
52	S52	0.1494	0.4133	-0.1103	0.01217

Table 5 Area of Soil Moisture derived from multi-spectral image.

Sl. No.	Soil moisture (Derived Multi spectral image)	Area in km2	(%) Area in km2
1.	0.1-0.16677(Very low)	10.9692	6.006574
2.	0.1678-0.3766(Low)	25.9155	14.19095
3.	0.3767-0.5234(Moderate)	52.209	28.58889
4.	0.5235-0.6645(High)	64.6335	35.39236
5.	0.6646-1.071(Very high)	28.8927	15.82122
	Total	182.6199	100

The following are some typical techniques for validating LU/LC generated from remote sensing: Crowdsourcing, statistical analysis, expert assessment, visual interpretation, and gathering real-world data. So, Validation of remote sensing derived LU/LC is essential for ensuring the accuracy and reliability of the derived data. A combination of the above methods can be used to validate the data, depending on the project requirements and available resources. The LU and LC map use in this project is generated from Sentinel-2A image unsupervised classification. For finding the special object in Bhagwanpur-I CD block, this map is very useful. This LU/LC image is classified into 5 categories as; water bodies, vegetation, fallow land, settlements and agricultural lands. The maximum area agricultural lands and vegetation are covered by 44.8907 % (15.4817km2), and 1.141228% (69.6432 km2) respectively they are mostly located in the middle and northern parts as well as the southern to western parts in the study. The lowest water bodies, fallow lands and settlements is covered 8.494303% (15.4817 km2), 1.141228% (2.08 km2) and 7.262819 % (13.2372 km2) respectively, maximum area water bodies that are found in the northern portion of the study that are extra water in the soil are shown in the figure (11) & table (6).

Table 6 LU/LC area of the study.

Sl. No.	LU/LC features name	Area in km2	% of area in km2
1.	Water bodies	15.4817	8.494303
2.	Vegetation	69.6432	38.21095
3.	Fallow land	2.08	1.141228
4.	Settlements	13.2372	7.262819
5.	Agricultural lands	81.8177	44.8907
	Total	182.2598	100

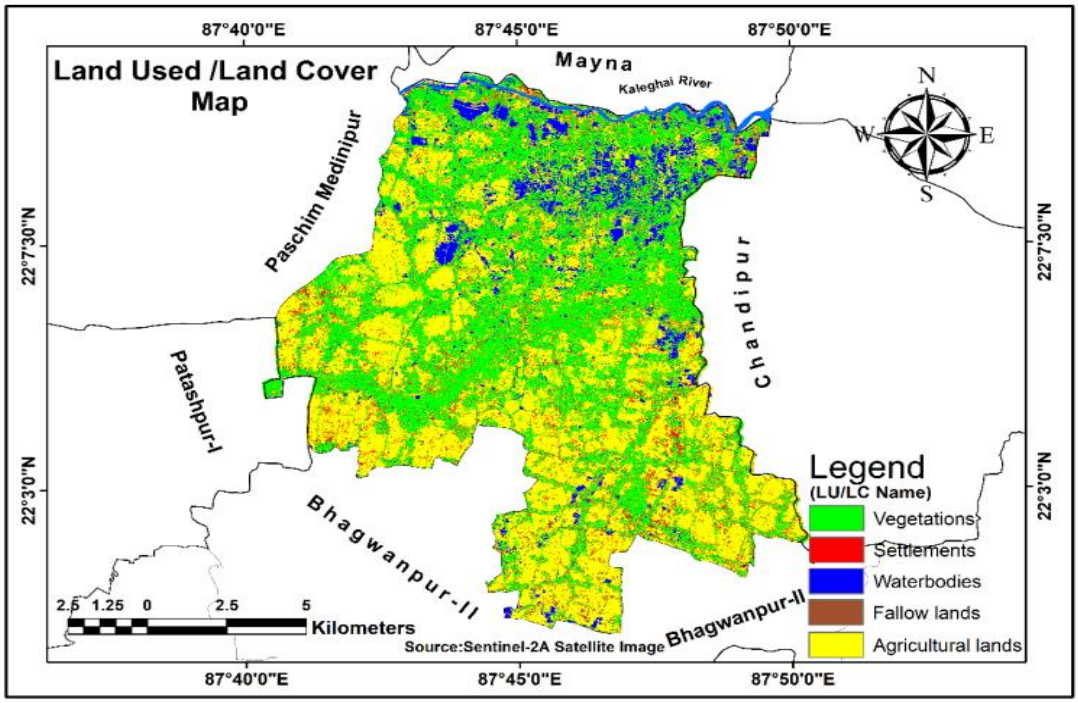

Fig. 11 LU and LC map of the study area.

Gravimetric Soil Moisture (GSM)

Gravimetric Soil Moisture (GSM) Map with the SSM (Surface Soil Moisture) map based on TVDI. While both maps provide information on soil moisture, they are based on different methods of measurement and therefore can have differences the values of soil moisture distribution in space. It is wealth observing that the GSM map was based on direct in-situ soil samples, it provides more accurate measurements of the soil moisture in the locations where soil samples were taken, but may not always accurately reflect the soil moisture levels across the research area. However, due to factors including cloud cover and soil type, the precision of the TVDI-based Surface Soil Moisture (SSM) map, which offers a more thorough assessment of soil moisture conditions across a greater area, may be questionable. In order to comprehend the soil moisture in the research region more completely, it is crucial to take into account both maps simultaneously. Figure 12 & Table 7.

Table 7 Area of Gravimetric soil moisture of the study area.

Sl. No.	Gravimetric Soil Moisture (%)	Area in km^2	% of Area in km^2
1.	2.12-9.12(Very low)	14.122	7.745
2.	9.13-12.30(Low)	38.773	21.264
3.	12.40-15.00(Moderate)	77.580	42.547
4.	15.10-18.60(High)	31.804	17.442
5.	18.70-27.30(Very high)	20.062	11.002
	Total	182.341	100.000

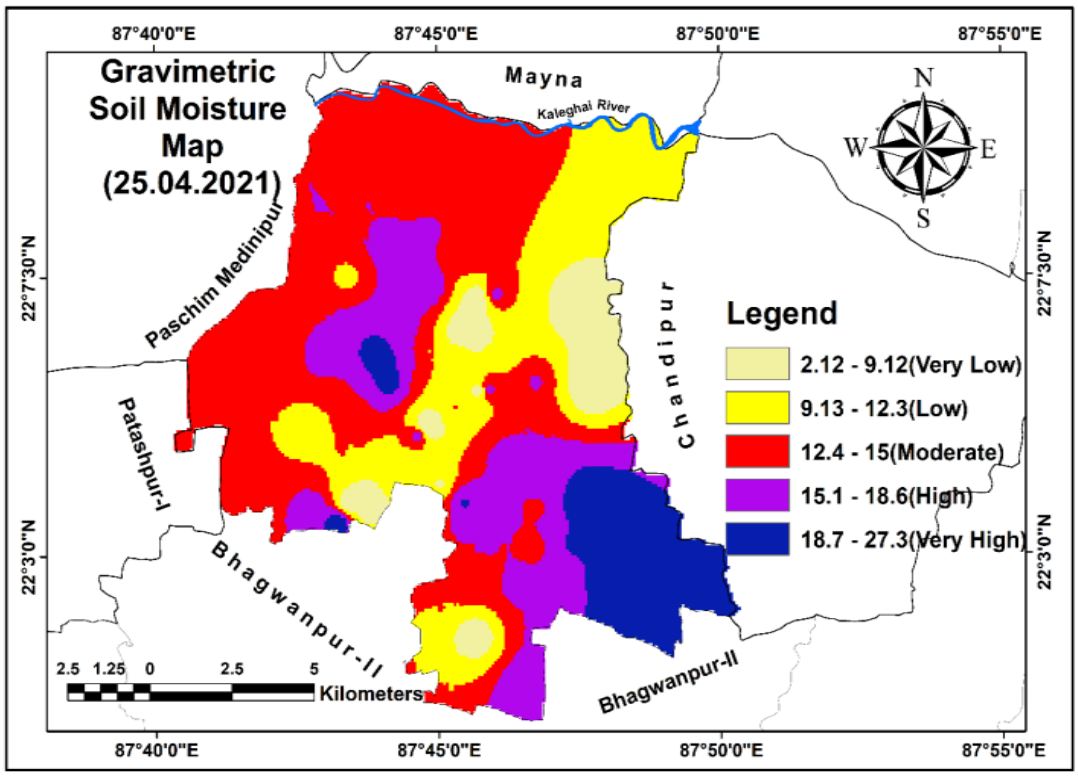

Fig. 12 Study area's gravimetric soil moisture map.

Soil moisture based on models (MBSM): The Model Based Soil Moisture (MBSM) Map was created by comparing in-situ soil moisture and backscattering coefficients. Very low, low, moderate, high, and very high were the resulting categories. According to the map, 11.922% (21.736 km2) of the study area has very low MBSM values, and 24.183% (44.089 km2) of the study area has low MBSM values. These values are primarily found in the study area's centre and western regions, where there is less water in the soil. The third type, moderate MBSM values, covers 31.857% (58.078 km2) of the area and is found in northern and some middle part in the study area where, the soil has a moderate amount of water. Lastly, the high and very high MBSM values cover 27.813% (50.706 km2) and 4.224% (7.700 km2) respectively, and are located in the south and southeast portion of the study area where there is very high-water content in the soil. Overall, the MBSM map delivers a valuable tool for understanding the variation of the soil moisture within the study area, which can have significant implications for agricultural and hydrological management (Figure 13 & Table 8).

Table 8 Area of Model based soil moister.

Sl. No.	MBSM Values	Area in sq.km	% of area in sq.km
1.	0.01111-0.0122(Very low)	21.736	11.922
2.	0.01221-0.01255(Low)	44.089	24.183
3.	0.011256-0.01289(Moderate)	58.078	31.857
4.	0.0129-0.0133(High)	50.706	27.813
5.	0.01332-0.01455(Very high)	7.700	4.224
	Total	182.308	100

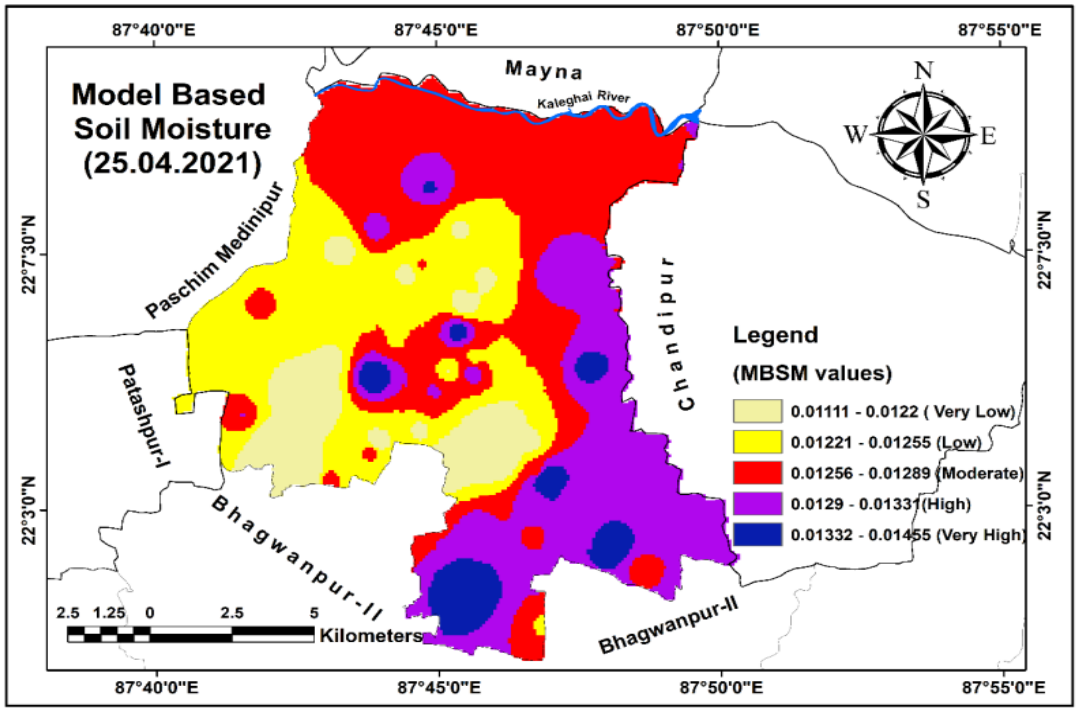

Fig. 13 Model Based Soil Moisture of the study area.

Relationship between Volumetric Soil Moisture Content and Gravimetric Soil Moisture (%): Two approaches that are frequently used to gauge how much water is present in soil are moisture content measured by gravity and soil moisture measured by volume. Volumetric soil moisture content is expressed as a percentage of the total soil volume, but gravimetric soil moisture is frequently expressed as a percentage of the dry weight of the soil. The relationship between these two measures of soil moisture can be complex and is influenced by a number of factors, including soil texture, porosity, and organic matter content. In the study, Gravimetric soil moisture and volumetric soil moisture content have a strong positive connection (R2=0.8548), with greater gravimetric soil moisture values often suggesting higher volumetric soil moisture content. This correlation can be quantified using various arithmetic procedures, which can be performed to control the nature, intensity, and direction of the link among the two variables (Figure (14) & Table (9)). However, it is crucial to keep in mind that the precise relationship between gravimetric soil moisture and volumetric soil moisture content might change based on the exact kind of soil and environmental factors in a given study region.

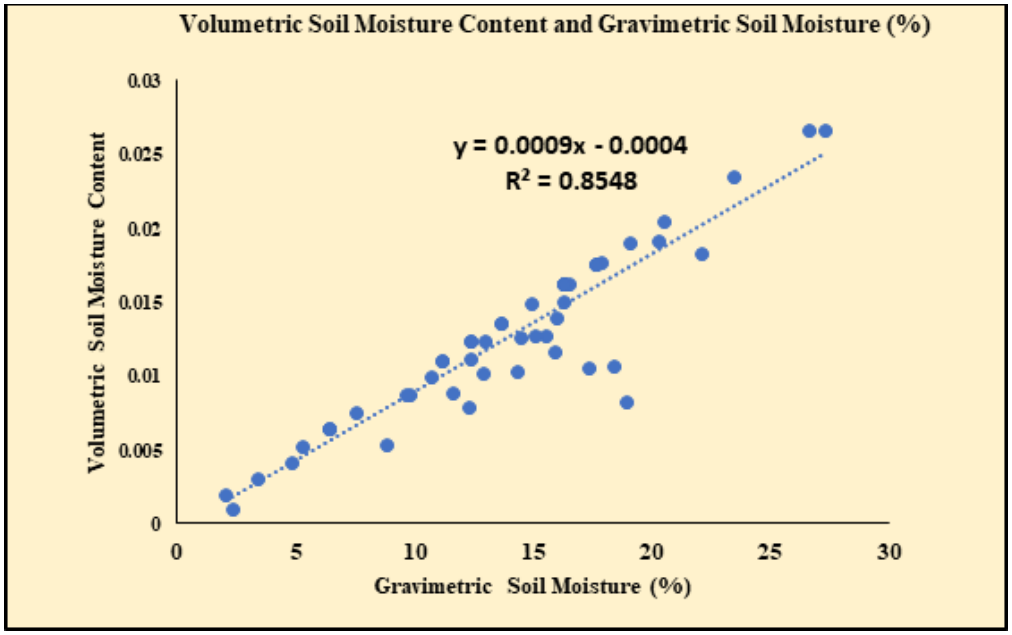

Fig. 14. Correlation between Gravimetric Soil Moisture (%) and Volumetric Soil Moisture Content of study area.

Table 9 Volumetric Soil Moisture Content and Volumetric Soil Moisture Content.

Sample Name	Latitude	Longitude	Gravimetric Soil Moisture (%)	Volumetric Soil Moisture Content
S1	22.02794	87.76105	6.382980	0.0064
S2	22.06251	87.71230	17.647100	0.0176
S3	22.01494	87.77608	17.857100	0.0177
S4	22.03250	87.81374	26.582300	0.0266
S5	22.05863	87.72033	23.456800	0.0235
S6	22.06425	87.72346	6.382980	0.0064
S7	22.09656	87.77899	15.493000	0.0127
S8	22.03529	87.80560	20.253200	0.0192
S9	22.09557	87.79541	3.370790	0.0031
S10	22.06330	87.72878	4.819280	0.0042
S11	22.06930	87.75054	8.771930	0.0054
S12	22.07376	87.74275	9.756100	0.0088
S13	22.08187	87.74395	16.279100	0.0163
S14	22.09651	87.73545	20.481900	0.0205
S15	22.10418	87.73248	22.058800	0.0183
S16	22.13114	87.75949	14.473700	0.0126
S17	22.13816	87.74437	17.647100	0.0176
S18	22.12044	87.73806	15.068500	0.0127
S19	22.12225	87.74745	18.367300	0.0107
S20	22.08798	87.72629	14.285700	0.0103
S21	22.10221	87.71631	16.470600	0.0163
S22	22.09183	87.71631	12.280700	0.0079
S23	22.08409	87.70897	11.594200	0.0089
S24	22.08426	87.71227	9.638550	0.0088
S25	22.07785	87.69099	13.636400	0.0136
S26	22.07147	87.69643	12.359600	0.0124

S27	22.04246	87.77573	16.279100	0.0163
S28	22.05298	87.77760	12.359600	0.0124
S29	22.05681	87.78276	16.279100	0.0163
S30	22.05322	87.78936	19.047600	0.0190
S31	22.06293	87.79429	27.272700	0.0267
S32	22.06869	87.77699	16.250000	0.0151
S33	22.06240	87.77819	13.636400	0.0136
S34	22.06396	87.76801	17.307700	0.0106
S35	22.06404	87.75783	18.918900	0.0083
S36	22.11053	87.73881	16.279100	0.0163
S37	22.14264	87.74379	12.857100	0.0102
S38	22.13301	87.73532	16.000000	0.0139
S39	22.10751	87.69966	12.941200	0.0124
S40	22.08963	87.75508	12.345700	0.0112
S41	22.10389	87.75682	10.714300	0.0100
S42	22.10994	87.75892	2.040820	0.0020
S43	22.11878	87.76181	5.263160	0.0053
S44	22.12009	87.76747	15.873000	0.0116
S45	22.11697	87.79117	6.382980	0.0064
S46	22.12513	87.72353	11.111100	0.0111
S47	22.08474	87.74718	2.325580	0.0010
S48	22.09460	87.76518	16.279100	0.0163
S49	22.09409	87.76180	7.526880	0.0075
S50	22.07573	87.77077	17.647100	0.0176
S51	22.09057	87.75966	11.111100	0.0111
S52	22.04653	87.75964	14.942500	0.0149

Conclusion

The Temperature Vegetation Dryness Index (TVDI) approach, which was used in the current study, was performed to estimate the soil moisture content in the upper layer of agricultural fields using optical data from a Landsat 8 satellite picture. Traditional methods for analysing direct in-situ methods were used to calculate the surface soil moisture. An accurate assessment of soil moisture using the TVDI method was established, and a significant association between LST and NDVI was found.

Through the regression study, the surface of TVDI was formed, which formerly associated with the gravimetric soil moisture. So, the results showed a positive association, indicating that the developed models worked well in the study area. The study's conclusions show how remote sensing data can provide estimates of actual surface soil moisture. The TVDI method, in particular, was found to be effective and can be used in conjunction with in-situ measurements to improve accuracy. The results have important implications for crop growing and hydrological resource management, as a precise measurement of surface soil moisture can help optimize irrigation and water use practices.

Acknowledgements

The author is thankful to Prof. Dr. Dipanwita Dutta kundu for guidance to carry out this work. Mr. Kousik Karmakar, former Remote Sensing and GIS expert, Bangalore, are thanked for helpful discussions during this work. I thank my student Ms. Maitry Das and Ms. Somasree Giri for assistance during field work.

References

Anguela, M.Zribi, F.Habets, S.Hasenauer, C.Loumagne. 2008. Analysis of surface and root soil moisture dynamics with ERS scatter meter and hydrometriological model SAFRAN-ISBAMODCOU at grand Morin watershed (france).Hydro. EarthSystem. Science.1903-926.

Anudeep, S. 2013. Blending approach for soil moisture retrieval using microwave remote sensing MTech dissertation, Andhra University, pp. 1–95). IIRS, ISRO, Dehradun.

Amato, F., Havel, J., Gad, A., El-Zeiny, A. 2015. Remotely Sensed Soil Data Analysis Using Artificial Neural Networks: A Case Study of El-Fayoum Depression. Egypt. ISPRS International Journal of Geo-Information 4 (2), 677–696.

Bauer-Marschallinger, B., Paulik, C., Hochstöger, S., Mistelbauer, T., Modanesi, S., Ciabatta, L., Massari, C., Brocca, L., Wagner, W. 2018. Soil moisture from data fusion of scatterometer and SAR: closing the scale gap with temporal filtering. Remote Sens. (Basel) 10, 1030.

Batlivala, P.P., Ulaby, F.T. 1977. Feasibility of monitoring soil moisture using active microwave remote sensing Remote Sensing Laboratory. Tech. Rep., 264–12, University of Kansas, Lawrence.

Bertoldi, G., Chiesa, S. D., Notarnicola, C., Pasolli, L., Niedrist, G., &Tappeiner, U. 2014. Estimation of soil moisture patterns in mountain grasslands by means of SAR RADARSAT2 images and hydrological modeling. Journal of Hydrology, 516, 245–257.

Chai, S. S., Walker, J. P., Makarynskyy, O., Kuhn, M., Veenendaal, B., & West, G. 2010. Use of soil moisture variability in artificial neural network retrieval of soil moisture. Remote Sensing, 2, 166–190.

Chan, S.K., Bindlish, R., O'Neill, P.E., Njoku, E., Jackson, T., Colliander, A., Chen, F., Burgin, M., Dunbar, S., Piepmeier, J., et al. 2016. Assessment of the SMAP passive soil moisture product. IEEE T Geosci. Remote 54, 4994–5007.

Das Goutam kumar. (2017). A Geo-Spatial analysis and Assessment of Groundwater Potential Zones by Using Remote Sensing and GIS Techniques-A micro level Study of Bhagwanpur-I CD Block in Purba Midnapur District, West Bengal, India. International Journal of Experimental Research and Review (IJERR). Int. J. Exp. Res. Rev., Vol. 14: 9-19.

Das Kousik and Paul Prabir Kumar. 2015. Present status of soil moisture estimation by microwave remote sensing. Cogent Geoscience.

Du,J.,Shi,J and Sun. 2010. The development of HJ SAR soil moisture retrieval algorithem.Int.J.Remo.Sens.,31 (14),3691-3705.

Hammam, A.A., Mohamed, E.S.2018. Mapping soil salinity in the East Nile Delta using several methodological approaches of salinity assessment. Egypt. J. Remote Sensing Space Science.

Hajji,M.E.,Baghdadi,N.,Zribi,M.,Belaud,G,Cheviron,B.,Courault,D. and Charron, F.2016. Soil Moisture retrieval over irrigated grassland using X-band SAR data. Remote Sensing of Environment,176,202-218.

Kornelsen, K.C., Coulibaly, P. 2013. Advances in soil moisture retrieval from synthetic aperture radar and hydrological applications. J. Hydrol. 476 (2013), 460–489.

Kornelsen, K. C., & Coulibaly, P. 2013. Advances in soil moisture retrieval from synthetic aperture radar and hydrological applications. Journal of Hydrology, 476, 460– 489.

Kurucu, Y.,BalickSanli, F.,Esetlili,M.T.,Bolca,M. and Goksel,C. 2009. Contribution of SAR images to determination of surface moisture on the Menemen plain, Turkey.Int.J.Remo.Sens.,30 (7),1805-1817.

Maiti, S.K. and Basak, B.B. 2013. Soil moisture regimes and their classification for crop planning in parts of Paschim Medinipur district of West Bengal. Journal of Crop and Weed, 9(2), pp.89-93.

Mandal Souvik, Roy Taniya. (2019).Evolution and Trend of Settlement Pattern Associate with General Physiography in Bhagwanpur-I CD Block. Thematics Journal of Geography, 8 (4). ISSN 2277-2995.

Mariapaola Ambrosonea, Alessandro Matesea, Salvatore Filippo Di Gennaroa, Beniamino Giolia, Marin Tudoroiub , Lorenzo Genesioa , Franco Miglietta , Silvia Barontia , Anita Maienzaa , FabrizioUngaroa , Piero Toscanoa.2020.Retrieving soil moisture in rainfed and irrigated fields

using Sentinel-2 observations and a modified OPTRAM approach. Int J Appl Earth Obs Geoinformation,

Petropoulos, G.P., Ireland, G., Barrett, B. 2015. Surface soil moisture retrievals from remote sensing: Current status, products and future trends. Phys. Chem. Earth (in press).

Prakash, R., Singh, D., & Pathak, N. P. 2012. A fusion approach to retrieve soil moisture with SAR and optical data. IEEE Journal of Selected Topics in Applied Earth Observations and Remote Sensing, 5, 196–206.

Rao NPV, Venkataratnam L, Rao KPV, Ramana KV, Singarao MN. 1993. Relation between root zone soil moisture and normalized difference vegetation index of vegetated fields. International Journal of Remote Sensing 14:441-9.

Ruszczak Bogdan, Mankoswska-Dominika.2022. Soil Moisture a Posteriori Measurements Enhancement Using Ensemble Learning. MDPI stays neutral with regard to jurisdictional claims in published maps and institutional affiliations.

Seneviratne, S.I., Corti, T., Davin, E.L., Hirschi, M., Jaeger, E.B., Lehner, I., Orlowski, B., Teuling, A.J. 2010. Investigating soil moisture-climate interactions in a changing climate: a review. Earth Sci. Rev. 99 (3-4), 125–161.

Şekertekin, A., Marangoz, A.M., Abdikan, S. 2016. Soil moisture mapping using Sentinel1A synthetic aperture radar data. Int. J. Environ. Geoinformatics. 5 (2), 178–188.

Sadeghi, M., Babaeian, E., Tuller, M., Jones, S.B. 2017. The optical trapezoid model: a novel approach to remote sensing of soil moisture applied to Sentinel-2 and Landsat-8 observations. Remote Sens. Environ. 198, 52–68.

Sandholt Inge, Rasmussen kjeld, Andersen Jens .2002. A simple interpretation of the surface temperature/vegetation index space for assessment of surface moisture status. Remote Sensing of Environment, 79, Issues 2–3, Pages 213-224.

Srivastava, H.S., Sharma, P. K, Kumar, D.,Sivankar,T.,Mishra,R.S.,Mishra, M. andpatel,P.2015.Soil Moisture Variation over the parts of Saharanpur and Haridwar districts (India) during November-2006 to June-2007 as observed by multi-polarized (VV/VH and VV/VH) ENVISAT-I temporal ASAR data. International Journal of Advanced Engineering Research and Science (IJAERS), 2(1), 31-39.

Sobrino A Jose, Juan C Jimenez-Munoz, Paolini Leonardo.2004. Land surface temperature retrieval from LANDSAT TM 5. Remote Sensing of Environment 90 (2004) 434 – 440.

Wang.R, geo. P, Zhou, Li and G. Y, Zhao. 2021.Experimental detection of the volume of the drip irrigation soil wetted body using Ground Penetrating Radar. Journal of Soil and Water Conservation May 2021, 76 (3) 199-210.

Xin, J., Tian, G., Liu, Q., Chen, L., 2006. Combining vegetation index and remotely sensed temperature for estimation of soil moisture in China. Int. J. Remote Sens. 27 (10), 2071–2075.

Zubair Younis Syed Muhammad, Iqbal Javed. 2015. Estimation of Soil Moisture Using Multispectral and FTIR techniques. National Authority for remote sensing and space Sciences.

Zribi, M., Sahnoun, M., Baghdadi, N., Toan, T. L, Hamida, A, B.2016.Analysis of the relationship between backscattered P-band radar signals and soil roughness. Remote sensing of Environment, 186, 13-21.

Citation

Das, G.K. (2024). Estimation of Surface Soil Moisture from Agricultural Lands using Multi-spectral Optical Satellite Data: A Study of Bhagwanpur-I CD Block, East Medinipur, West Bengal, India. In: Dandabathula, G., Bera, A.K., Rao, S.S., Srivastav, S.K. (Eds.), Proceedings of the 43rd INCA International Conference, Jodhpur, 06–08 November 2023, pp. 84–108, ISBN 978-93-341-2277-0.